Null-field integral equation approach for Helmholtz (interior and exterior acoustic) problems with circular boundaries

Chia-Tsung Chen[1], I-Lin Chen[2], Jeng-Tzong chen[3]

Key words: null-field integral equation, singular value decomposition, degenerate kernel, Fourier series, Helmholtz, radiation, scattering.

Abstract

The Helmholtz (interior and exterior acoustics) problems with circular boundaries are studied by using the null-field integral equations in conjunction with degenerate kernels and Fourier series to avoid calculating the Cauchy and Hadamard principal values. Adaptive observer system of polar coordinate is considered to fully employ the property of degenerate kernels. For the hypersingular equation, vector decomposition for the radial and tangential gradient of potential is carefully considered. In interior acoustic problems, direct-searching scheme is employed to detect the eigenvalues by using the singular value decomposition (SVD) technique. Two approaches to overcome spurious eigenvalus, SVD updating technique and Burton & Miller methods are employed to suppress the appearance of spurious eigenvalue. Several examples are demonstrated to see the validity of the present formulation and numerical results indicate the better accuracy than BEM in predicting the spurious eigenvalues. In exterior acoustic problems, the radiation and scattering problems with multiple circular cylinders are also examined successfully.

零場積分方程法求解赫姆茲(內外域聲場)含圓形邊界問題

陳佳聰[1], 陳義麟[2], 陳正宗[3]

關鍵詞：零場積分方程、奇異值分解、退化核(分離核)、傅立葉級數、赫姆茲、輻射、散射。

摘要

本文使用零場積分方程，搭配退化核(分離核)及傅立葉級數來解決含圓形邊界的赫姆茲(內外域聲)問題以避免柯西及哈達馬主值的計算。自適性觀察的極座標系統可充分

[1]Graduate student, Department of Harbor and River Engineering, National Taiwan Ocean University
[2]Associate professor, Department of Naval Architecture, National Kaohsiung Marine University
[3] Distinguished professor, Department of Harbor and River Engineering, National Taiwan Ocean University

展現退化核(分離核)的特性。而在使用超奇異式時，對勢能場的法線及切線方向的向量分解均必須小心處理。在內域聲場問題，直接使用奇異值分解技巧，可求得特徵值與特徵模態。為了克服假根問題，我們使用 SVD 補充行與補充列法 及 Burton & Miller 法可克服假根產生的問題。幾個例子驗證了本方法的正確性。數值結果顯示，本方法對於假根所預測座落的位置比邊界元素法更為精確。在外域聲場問題，含多圓柱的輻射及散射問題都已測試成功。

1. Introduction

For acoustic problem, it is well known that the boundary integral equation method (BIEM) in solving the exterior and interior problems results in fictitious frequency and spurious eigenvalue, respectively. The nonuniqueness problem is numerically manifested in a rank deficiency of the coefficient matrix in BEM. Spurious eigenvalues appear when the influence matrix is rank deficient in the case where physical response does not occur. Fictitious frequency results in numerical resonance but physical resonance never occurs for exterior problems. In order to obtain the unique solution, various integral equation formulations that provide additional constraints to the original system of equations have been proposed. Burton & Miller proposed an integral equation that was valid for all wavenumbers; however, the calculation for the hypersingular integration is required. To avoid the computation of hypersingularity, an alternative method, CHIEF, was proposed by Schenck [5]. Recently, the SVD technique was developed as an important tool in linear algebra. In the interior eigenproblem with a simply-connected domain, the dual reciprocity method (DRM) by Partridge *et al.* [4] and the multiple reciprocity method (MRM) by Kamiya & Andoh [3] have been widely used recently. In exterior acoustics, many researchers applied the CHIEF method to deal with the problem of fictitious frequencies. Schenck used the CHIEF method which employed the boundary integral equations by collocating the interior point as an auxiliary condition to make up deficient constraint condition. The constraint is one of the null-field integral equations. In this paper, we employ the null-field integral equation (NFIE) as well as the boundary integral equation method (BIEM) in conjunction with degenerate kernels and Fourier series to solve the vibration of multiply-domain membrane and the radiation and scattering problems with circular boundaries. To fully utilize the geometry of circular boundary, Fourier series for boundary densities and degenerate kernel for fundamental solutions are incorporated into the null-field integral equation in the polar coordinate system.

2. Problem Statement and Integral Formulation

2.1 Problem statement

The governing equation of the acoustic problem is the Helmholtz equation

$$(\nabla^2 + k^2)u(x) = 0, \quad x \in D, \tag{1}$$

where ∇^2, k and D are the Laplacian operator, the wave number, and the domain of interest, respectively. Consider the problems containing N randomly distributed circular holes centered at the position vector c_j (j =1, 2, ..., N) as shown in Figure 1.

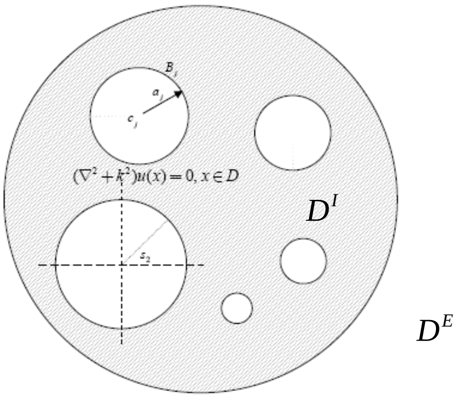

Figure 1 Problem statement

2.2 Dual boundary integral formulation

Based on the dual boundary integral formulation of the domain point [1], we have

$$2\pi u(x)=\int_B T(s,x)u(s)dB(s)-\int_B U(s,x)t(s)dB(s),\ x\in D^I, \qquad (2)$$

$$2\pi t(x)=\int_B M(s,x)u(s)dB(s)-\int_B L(s,x)t(s)dB(s),\ x\in D^I, \qquad (3)$$

where s and x are the source and field points, respectively, D^I is the domain of the interests, $t(s)$ is the directional derivative of $u(s)$ along the outer normal direction at s. The $U(s,x)$, $T(s,x)$, $L(s,x)$ and $M(s,x)$ represent the four kernel functions [1].

2.3 Null-field integral formulation in conjunction the degenerate kernel and Fourier series

By collocating x outside the domain ($x\in D^E$), we obtain the null-field integral equations as shown below [1]:

$$0=\int_B T(s,x)u(s)dB(s)-\int_B U(s,x)t(s)dB(s),\ x\in D^E, \qquad (4)$$

$$0=\int_B M(s,x)u(s)dB(s)-\int_B L(s,x)t(s)dB(s),\ x\in D^E. \qquad (5)$$

In the real computation, we select the null-field point x on the boundary. By using the polar coordinate, we can express $x=(\rho,\phi)$ and $s=(R,\theta)$. The four kernels, U, T, L and M can be expressed in terms of degenerate kernels as shown below [1]:

$$U(s,x)=\begin{cases} U^I(s,x)=\dfrac{-\pi i}{2}\displaystyle\sum_{m=-\infty}^{\infty} J_m(k\rho)H_m^{(1)}(kR)\cos(m(\theta-\phi)),\ R\ \geq\ \rho \\ U^E(s,x)=\dfrac{-\pi i}{2}\displaystyle\sum_{m=-\infty}^{\infty} H_m^{(1)}(k\rho)J_m(kR)\cos(m(\theta-\phi)),\ \rho>R \end{cases}, \qquad (6)$$

$$T(s,x)=\begin{cases} T^I(s,x)=\dfrac{-\pi ki}{2}\displaystyle\sum_{m=-\infty}^{\infty} J_m(k\rho)H_m'^{(1)}(kR)\cos(m(\theta-\phi)),\ R>\rho \\ T^E(s,x)=\dfrac{-\pi ki}{2}\displaystyle\sum_{m=-\infty}^{\infty} H_m^{(1)}(k\rho)J_m'(kR)\cos(m(\theta-\phi)),\ \rho>R \end{cases}, \qquad (7)$$

$$L(s,x)=\begin{cases} L^I(s,x)=\dfrac{-\pi ki}{2}\displaystyle\sum_{m=-\infty}^{\infty} J_m'(k\rho)H_m^{(1)}(kR)\cos(m(\theta-\phi)),\ R>\rho \\ L^E(s,x)=\dfrac{-\pi ki}{2}\displaystyle\sum_{m=-\infty}^{\infty} H_m'^{(1)}(k\rho)J_m(kR)\cos(m(\theta-\phi)),\ \rho>R \end{cases}, \qquad (8)$$

$$M(s,x)=\begin{cases} L^I(s,x)=\dfrac{-\pi k^2 i}{2}\displaystyle\sum_{m=-\infty}^{\infty} J_m'(k\rho)H_m'^{(1)}(kR)\cos(m(\theta-\phi)),\ R\ \geq\ \rho \\ L^E(s,x)=\dfrac{-\pi k^2 i}{2}\displaystyle\sum_{m=-\infty}^{\infty} H_m'^{(1)}(k\rho)J_m'(kR)\cos(m(\theta-\phi)),\ \rho>R \end{cases}, \qquad (9)$$

where $i^2=-1$, I and E denote the interior and exterior cases for the expressions of kernel, respectively. It is noted that the degenerate kernels for T and L expression for $\rho=R$ are not given since they are not continuous across the boundary.

In order to fully utilize the geometry of circular boundary, the potential u and its normal flux t can be approximated by employing the Fourier series. Therefore, we obtain

$$u(s) = a_0 + \sum_{n=1}^{\infty}(a_n \cos n\theta + b_n \sin n\theta),\ s \in B, \qquad (10)$$

$$t(s) = p_0 + \sum_{n=1}^{\infty}(p_n \cos n\theta + q_n \sin n\theta),\ s \in B, \qquad (11)$$

where a_0, a_n, b_n, p_0, p_n and q_n are the Fourier coefficients and θ is the polar angle which is equally discretized. Eqs. (4) and (5) can be easily calculated by employing the orthogonal property of Fourier series. In the real computation, only the finite M terms are used in the summation of Eqs. (10) and (11).

2.4 Adaptive observer system

Since the boundary integral equations are frame indifferent, *i.e.* rule of objectivity is obeyed. Adaptive observer system is chosen to fully employ the property of degenerate kernels. Figure 2 shows the boundary integration for the circular boundaries. It is worthy noted that the origin of the observer system can be adaptively located on the center of the corresponding circle under integration to fully utilize the geometry of circular boundary. The dummy variable in the integration on the circular boundary is just the angle (θ) instead of the radial coordinate (R). By using the adaptive system, all the boundary integrals can be determined analytically free of principal value.

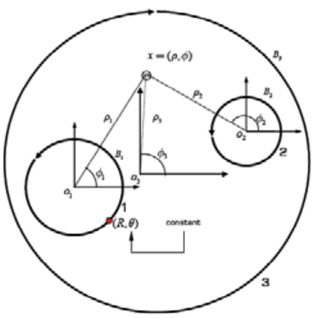

Figure 2 Adaptive observer system

2.5 Vector decomposition technique for the potential gradient in the hypersingular formulaion

Since the hypersingular equation is a key ingredient to deal with fictitious frequency, potential gradient on the boundary is required to calculate. For the encentric case, special treatment for the potential gradient should be taken care as the source point and field point locate on different circular boundaries. Special treatment for the normal derivative should be taken care. As shown in Figure 3 where the origins of observer system are different, the true normal direction $\hat{e}_1$ with respect to the collocation point x on the B_j boundary should be superimposed by using the radial direction $\hat{e}_3$ and angular direction $\hat{e}_4$. We call this treatment "vector decomposition technique". According to the concept, Eqs. (8) and (9) can be modified as

$$L(s,x) = \begin{cases} L^I(s,x) = \dfrac{-\pi k i}{2}\displaystyle\sum_{m=-\infty}^{\infty} J'_m(k\rho)H_m^{(1)}(kR)\cos(m(\theta-\phi))\cos(\phi_c-\phi_j) \\ \qquad -\dfrac{m}{k\rho}J_m(k\rho)H_m^{(1)}(kR)\sin(m(\theta-\phi))\sin(\phi_c-\phi_j),\ R>\rho \\ L^E(s,x) = \dfrac{-\pi k i}{2}\displaystyle\sum_{m=-\infty}^{\infty} H_m^{\prime(1)}(k\rho)J_m(kR)\cos(m(\theta-\phi))\cos(\phi_c-\phi_j) \\ \qquad -\dfrac{m}{k\rho}J_m(k\rho)H_m^{(1)}(kR)\sin(m(\theta-\phi))\sin(\phi_c-\phi_j),\ \rho>R \end{cases}, \qquad (12)$$

$$M(s,x) = \begin{cases} M^I(s,x) = \dfrac{-\pi k i}{2}\displaystyle\sum_{m=-\infty}^{\infty} J'_m(k\rho)H_m^{\prime(1)}(kR)\cos(m(\theta-\phi))\cos(\phi_c-\phi_j) \\ \qquad -\dfrac{m}{k\rho}J_m(k\rho)H_m^{\prime(1)}(kR)\sin(m(\theta-\phi))\sin(\phi_c-\phi_j),\ R \ge \rho \\ M^E(s,x) = \dfrac{-\pi k i}{2}\displaystyle\sum_{m=-\infty}^{\infty} H_m^{\prime(1)}(k\rho)J'_m(kR)\cos(m(\theta-\phi))\cos(\phi_c-\phi_j) \\ \qquad -\dfrac{m}{k\rho}J_m(k\rho)H_m^{\prime(1)}(kR)\sin(m(\theta-\phi))\sin(\phi_c-\phi_j),\ \rho>R \end{cases}. \qquad (13)$$

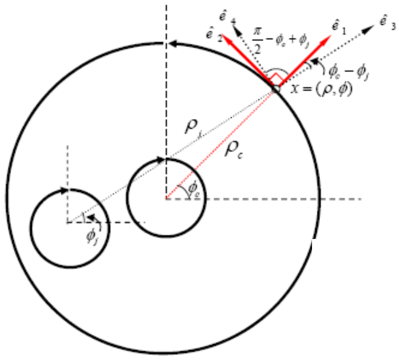

Figure 3 Vector composition

2.6 Linear Algebraic Equation

In order to calculate the 2M+1 unknown Fourier coefficients and 2M+1 boundary points on each circular boundary are needed to be collocated. By moving the null-field point to the kth circular boundary for Eqs. (4) and (5) as shown in Figure 4, we have

$$0=\sum_{j=1}^{N_c}\int_{B_j}T(s,x_k)u(s)dB_j(s)-\sum_{j=1}^{N_c}\int_{B_j}U(s,x_k)t(s)dB_j(s),\ x_k\in D^E, \tag{14}$$

$$0=\sum_{j=1}^{N_c}\int_{B_j}M(s,x_k)u(s)dB_j(s)-\sum_{j=1}^{N_c}\int_{B_j}L(s,x_k)t(s)dB_j(s),\ x_k\in D^E, \tag{15}$$

where N_c is the number of circles. It is noted that the path is anticlockwise for the outer circle. Otherwise, it is clockwise. For the B_j integral of the circular boundary, the kernels of $U(s,x)$, $T(s,x)$ $L(s,x)$ and $M(s,x)$ are respectively expressed in terms of degenerate kernels of Eqs. (6), (7), (12) and (13) with respect to the observer origin at the center of B_j. The boundary densities of $u(s)$ and $t(s)$ are substituted by using the Fourier series of Eqs. (10) and (11), respectively. In the B_j integration, we set the origin of the observer system to collocate at the center c_j of B_j to fully utilize the degenerate kernel and Fourier series. By moving the null-field point which can be much close to the boundary B_k from outside of the domain, a linear algebraic system is obtained

$$[\boldsymbol{U}]\{\boldsymbol{t}\}=[\boldsymbol{T}]\{\boldsymbol{u}\}, \tag{16}$$

$$[\boldsymbol{L}]\{\boldsymbol{t}\}=[\boldsymbol{M}]\{\boldsymbol{u}\}, \tag{17}$$

where $[\boldsymbol{U}]$, $[\boldsymbol{T}]$, $[\boldsymbol{L}]$ and $[\boldsymbol{M}]$ are the influence matrices with a dimension of $N_c(2M+1)$ by $N_c(2M+1)$ and $\{\boldsymbol{t}\}$ and $\{\boldsymbol{u}\}$ denote the vectors for $t(s)$ and $u(s)$ of the Fourier coefficients with a dimension of $N_c(2M+1)$ by 1. where, $[\boldsymbol{U}]$, $[\boldsymbol{T}]$, $[\boldsymbol{L}]$, $[\boldsymbol{M}]$, $\{\boldsymbol{u}\}$ and $\{\boldsymbol{t}\}$ can be defined as follows:

$$[\boldsymbol{U}]=[\boldsymbol{U}_{\alpha\beta}]=\begin{bmatrix}\boldsymbol{U}_{00} & \boldsymbol{U}_{01} & \cdots & \boldsymbol{U}_{0N}\\ \boldsymbol{U}_{10} & \boldsymbol{U}_{11} & \cdots & \boldsymbol{U}_{1N}\\ \vdots & \vdots & \ddots & \vdots\\ \boldsymbol{U}_{N0} & \boldsymbol{U}_{N1} & \cdots & \boldsymbol{U}_{NN}\end{bmatrix}, \tag{18}$$

$$[\boldsymbol{T}]=[\boldsymbol{T}_{\alpha\beta}]=\begin{bmatrix}\boldsymbol{T}_{00} & \boldsymbol{T}_{01} & \cdots & \boldsymbol{T}_{0N}\\ \boldsymbol{T}_{10} & \boldsymbol{T}_{11} & \cdots & \boldsymbol{T}_{1N}\\ \vdots & \vdots & \ddots & \vdots\\ \boldsymbol{T}_{N0} & \boldsymbol{T}_{N1} & \cdots & \boldsymbol{T}_{NN}\end{bmatrix}, \tag{19}$$

$$[\boldsymbol{L}]=[\boldsymbol{L}_{\alpha\beta}]=\begin{bmatrix}\boldsymbol{L}_{00} & \boldsymbol{L}_{01} & \cdots & \boldsymbol{L}_{0N}\\ \boldsymbol{L}_{10} & \boldsymbol{L}_{11} & \cdots & \boldsymbol{L}_{1N}\\ \vdots & \vdots & \ddots & \vdots\\ \boldsymbol{L}_{N0} & \boldsymbol{L}_{N1} & \cdots & \boldsymbol{L}_{NN}\end{bmatrix}, \tag{20}$$

$$[\boldsymbol{M}]=\left[\boldsymbol{M}_{\alpha\beta}\right]=\begin{bmatrix}\boldsymbol{M}_{00} & \boldsymbol{M}_{01} & \cdots & \boldsymbol{M}_{0N}\\ \boldsymbol{M}_{10} & \boldsymbol{M}_{11} & \cdots & \boldsymbol{M}_{1N}\\ \vdots & \vdots & \ddots & \vdots\\ \boldsymbol{M}_{N0} & \boldsymbol{M}_{N1} & \cdots & \boldsymbol{M}_{NN}\end{bmatrix}, \qquad (21)$$

$$\{\boldsymbol{u}\}=\begin{Bmatrix}\boldsymbol{u}_0\\ \boldsymbol{u}_1\\ \boldsymbol{u}_2\\ \vdots\\ \boldsymbol{u}_N\end{Bmatrix}, \{\boldsymbol{t}\}=\begin{Bmatrix}\boldsymbol{t}_0\\ \boldsymbol{t}_1\\ \boldsymbol{t}_2\\ \vdots\\ \boldsymbol{t}_N\end{Bmatrix}, \qquad (22)$$

where the vectors $\{\boldsymbol{u}_k\}$ and $\{\boldsymbol{t}_k\}$ are in the form of $\{a_0^k \ a_1^k \ b_1^k \ \cdots \ a_M^k \ b_M^k\}^T$ and $\{p_0^k \ p_1^k \ q_1^k \ \cdots \ p_M^k \ q_M^k\}^T$; the first subscript “α” ($\alpha = 0,1,2...,N$) in the $\left[\boldsymbol{U}_{\alpha\beta}\right]$ denotes the index of the αth circle where the collocation point is located and the second subscript “β” ($\beta = 0,1,2...,N$) denotes the index of the βth circle where the boundary data $\{\boldsymbol{u}_k\}$ or $\{\boldsymbol{t}_k\}$ are specified. N is the number of circular holes in the domain and M indicates the highest harmonic of truncated terms in Fourier series. The coefficient matrix of the linear algebraic system is partitioned into blocks, and each diagonal block (U_{pp}, p is no sum) corresponds to the influence matrices due to the same circle of collocation and Fourier expansion.

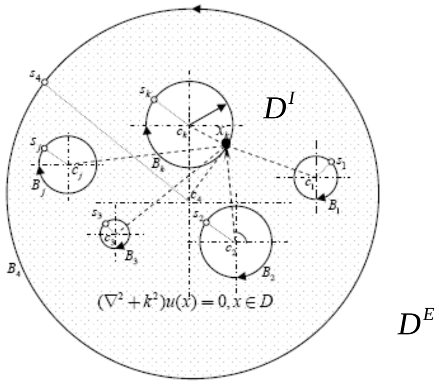

Figure 4 Null-field integral equation (x move to B from D^E)

3. Illustrative Example

Example1 Membrane vibration for a circular domain with an eccentric circular hole

An eccentric case with radii r_1 and r_2 ($r_1 = 0.5, r_2 = 2.0$) is considered as shown in Figure 5. The boundary condition is subject to the Dirichlet type. Special treatment for vector decompositions in potential gradient should be taken care here. Figure 6(a) shows the minimum singular value versus k where the drop indicates the possible eigenvalues by using the singular formulation. Figure 6 (b) shows the minimum singular value versus k where the drop indicates the possible eigenvalues by using the hypersingular formulation. Figure 6(c) shows the minimum singular value versus k where the drop indicates all the true eigenvalues by using the Burton & Miller approach. The present method by using the singular formulation agree with the analytical results better than BEM [1] does where a spurious eigenvalue appears at $k = 4.81$ ($J_0(4.81r_1) = 0$) instead of 4.83 in BEM. The present method by using the hypersingular formulation agree with the analytical solution better than BEM [1] does where a spurious eigenvalue appears at

$k = 0.0$ and 3.68 ($J_0'^1(0r_1) = 0$ and $J_0'^2(3.68r_1) = 0$) instead of 0.35 and 3.77 in BEM. The present method is superior to BEM especially in the low frequency range and it is more accurate than BEM under the same number of degree of freedoms. The spurious eigenvalue was filtered out by using the Burton and Miller approach [1]. By adopting the truncated Fourier series (M=10), the first five mode shapes are compared well with those by FEM and BEM also shown in Table 1.

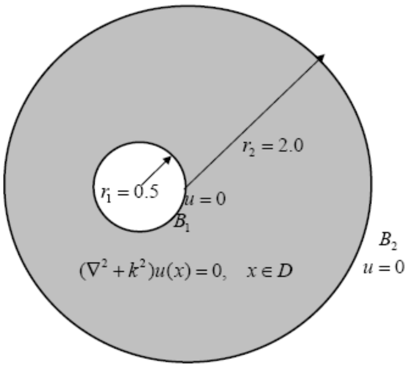

Figure 5 Eigenproblem with an eccentric domain

(a)
(b)
(c)

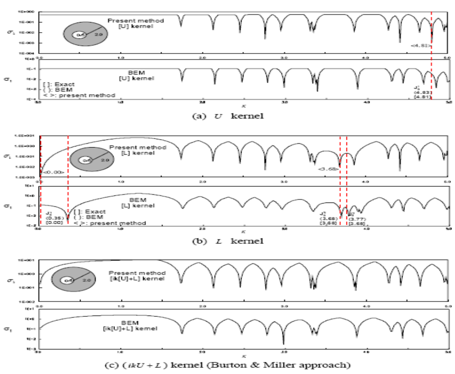

Figure 6 The minimim singular value σ_1 versus k f by using the present method and BEM

Mode	Present method (M=10)	BEM[27]	FEM[27]
1	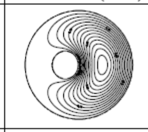	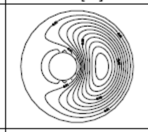	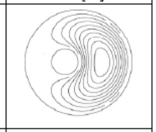
	$k = 1.74$	$k = 1.74$	$k = 1.74$
2	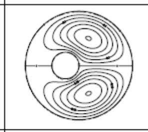	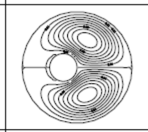	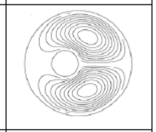
	$k = 2.14$	$k = 2.14$	$k = 2.13$
3	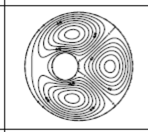	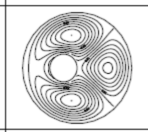	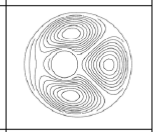
	$k = 2.46$	$k = 2.47$	$k = 2.45$
4	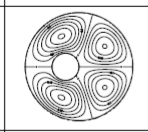	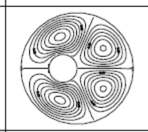	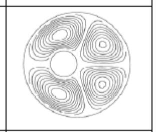
	$k = 2.78$	$k = 2.78$	$k = 2.76$
5	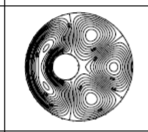	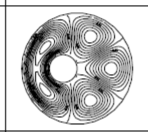	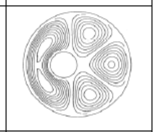
	$k = 2.94$	$k = 2.97$	$k = 2.95$

Table 1 The first five eigenmodes by using the present method, FEM and BEM.

Example 2 Scattering problem for five scatters (Dirichlet boundary condition)

Plane wave scattering by five soft circular cylinders (Dirichlet boundary condition) is considered in Figure 7. This problem was solved by using the multiple DtN approach [2]. Figure 8 shows the contour plots of the real part of potential for $k = \pi$. In Figure 9, there are no irregular frequencies by using present method but irregular frequencies occur by using BEM.

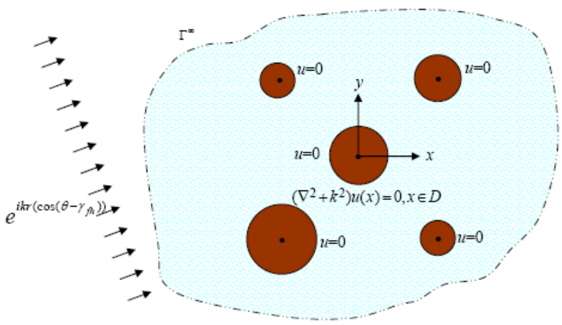

Figure 7 The palne wave scattering by five circular cylinders

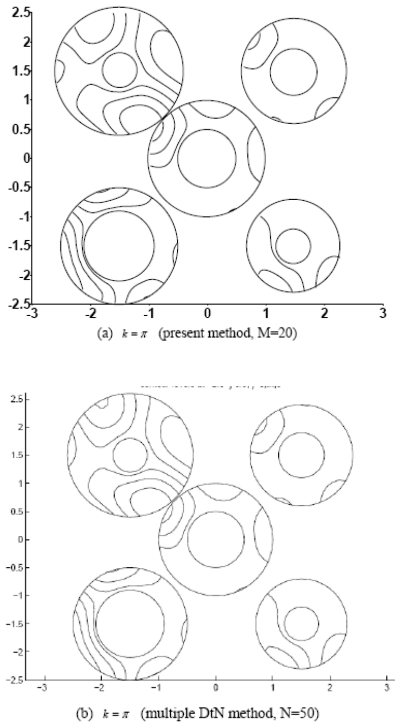

Figure 8 The contour plot of the real-part solutions of total field for $k=\pi$.

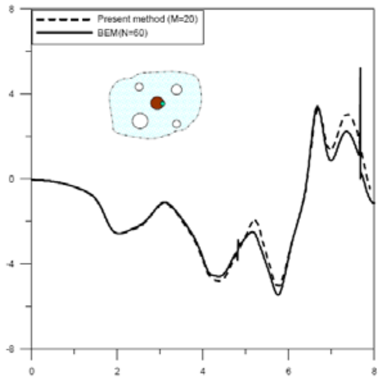

Figure 9 The positions of irregular values using different methods of center circle.

4. Concluding remark

This paper emphasized on interior eigenproblems of multiply-connected problems and multiple radiators and scatters by using the null-field integral equation approach in which degenerate kernels and Fourier series are employed. A systematic way to solve the Helmholtz problems with circular boundaries was proposed successfully in this paper by using the null-field integral equation in conjunction with degenerate kernels and Fourier series. Problems were examined to check the accuracy of the present formulation for engineering applications including free vibration of membrane and scattering of circular obstacles. All the numerical results were compared with BEM and FEM solutions. Good agreements were made.

References

1. Chen I. L., Chen J. T., Kuo S. R. and Liang M. T. (2001), A new method for true and spurious eigensolutions of arbitrary cavities using the CHEEF method, J. Acou. Soc. Amer. 109 982-999.
2. Grote M. J. and Kirsch C. (2004), Dirichlet to Neumann boundary conditions for multiple scattering problems, J. Comp. Physics 201 630-650.
3. Kamiya N. and Andoh E. (1993), A note on multiple reciprocity integral formulation for Helmholtz equation, Comm. Num. Meth. Engng. 9 9-13.
4. Partridge P. W., Brebbia C. A. and Wrobel L. C. (1992), The dual reciprocity boundary element method, Southampton: Comp. Mech. Publ.
5. Schenck H. A. (1968), Improved integral formulation for acoustic radiation problem, J. Acoust. Soc. Am. 44 41-58.
6. Chen C. T. (2005), Null-field integral equation approach for Helmholtz (interior and exterior acoustic) problems with circular boundaries, Master thesis, Taiwan Ocean University, Keelung.